Int. J. Bio-Inorg. Hybr. Nanomater., 4(3): 141-153, Autumn 2015

Organic template-free synthesis of Ni-ZSM-5 nanozeolite: a novel catalyst for formaldehyde electrooxidation onto modified Ni-ZSM-5/CPE

M. Rahimnejad[1]; S.K. Hassaninejad-Darzi[2]*

[1] Biofuel & Renewable Energy Research Center, Faculty of Chemical Engineering, Babol University of Technology, Babol, Iran.P.O.Box: 47148-71167
[2] Research Laboratory of Analytical & Organic Chemistry, Department of Chemistry, Faculty of Science, Babol University of Technology, Babol, Iran

Received: 26 May 2015; Accepted: 29 July 2015

ABSTRACT: A novel modified Ni-ZSM-5 nanozeolite was fabricated via an organic template-free hydrothermal route. The average particle size of Ni-ZSM-5 nanozeolite was calculated to be 85 nm by scanning electronic microscopy. Then, Carbon paste electrode (CPE) was modified by Ni-ZSM-5 nanozeolite and Ni^{2+} ions were then incorporated to the nanozeolite matrix. Electrochemical behavior of this electrode was investigated by cyclic voltammetry that exhibits stable redox behavior of Ni(III)/Ni(II) couple in alkaline medium. It has been shown that Ni-ZSM-5 nanozeolite at the CPE surface can improve catalytic efficiency of the dispersed nickel ions toward formaldehyde (HCHO) electrocatalytic oxidation. The values of electron transfer coefficient, charge-transfer rate constant and the electrode surface coverage were obtained to be 0.49, 0.045 s^{-1} and 4.11×10^{-8} mol cm^{-2}, respectively. Also, the catalytic rate constant for HCHO and redox sites of electrode and diffusion coefficient were found to be 9.064×10^{3} cm^{3} mol^{-1} s^{-1} and 8.575×10^{-6} cm^{2} s^{-1}, respectively.

Keywords: *Carbon paste electrode (CPE); modified electrode; Electrocatalysis; Formaldehyde; Ni-ZSM-5 nanozeolite; Template-free synthesis*

INTRODUCTION

Recently, electrocatalytic oxidation of small organic molecules such as CH_3OH, C_2H_5OH, HCHO and HCOOH, on the surface of different modified electrodes has received special attention. They have great potential for utilization as electron donors in fuel cells (FCs) and production of high current and power density (Ojani, *et al.*, 2013, Mai, *et al.*, 2005). Formaldehyde (HCHO) is toxic material and is not very suitable electron donors for FCs but study of its electrochemical oxidation is important for a full understanding of methanol oxidation in FCs. HCHO is also one of the intermediate products in methanol oxidation in FCs (Samjeske, *et al.*, 2007). HCHO is also used in textile industry and thus, its oxidation is relevant to waste water treatment (Santos and Bulhoes, 2004). Therefore, HCHO oxidation has been performed on different electrodes such as platinum and platinum alloys (Santos and Bulhoes, 2004, Korzeniewski and Childers, 1998, Miki, *et al.*, 2004, De Lima, *et al.*, 2007, Jiang, *et al.*, 2009, Habibi and Delnavaz, 2010, Mascaro, *et al.*, 2004, Li, *et al.*, 2011), copper and copper alloys (Ramanauskas, *et al.*,

(*) Corresponding Author - e-mail: rahimnejad@nit.ac.ir

1997, Raoof, *et al.*, 2012, Brunelli, *et al.*, 2002, Raoof, *et al.*, 2011), gold (Vaskelis, *et al.*, 2007, Yahikozawa, *et al.*, 1992, Yang, *et al.*, 1999), palladium nanoparticles (Safavi, *et al.*, 2009, Zhu, *et al.*, 2009, Gao, *et al.*, 2006, Yi, *et al.*, 2011, Zhang, *et al.*, 1997), gold alloy (Enyo, *et al.*, 1985), nickel based electrodes (Ojani, *et al.*, 2009, Aal, *et al.*, 2008, Raoof, *et al.*, 2011, Raoof, *et al.*, 2012, Raoof, *et al.*, 2009), nickel and copper alloy (Enyo, 1986).

Fabrication of modified electrodes for electro catalysis has been extensively developed and investigated by several researchers. Improvement in electrodes provides an excellent way to accelerate charge transfer, decrease the over potentials as well as increase the intensity of the corresponding voltammetric responses (Samadi-Maybodi, *et al.*, 2013). Zeolites and nanozeolites are ordered porous crystalline materials with different practical applications (Nejad-Darzi *et al.*, 2013). Surface areas for these materials is high, with strongly organized microporouse channel systems that exhibits an advantage over other classical support materials which are of high interest in FC technology (Li, *et al.*, 2002). Certain organic templates are usually necessary to be used as charge balancing and structure directing agent to obtain highly crystallized zeolites (Cundy and Cox, 2005). However, there are clear disadvantages for the organic template-contained synthesis, such as relatively high cost and environmental pollution (Song, *et al.*, 2006, Zhang, *et al.*, 2012). Improvement of new ways for fabrication of zeolites in absence of organic template is attractive (Nejad-Darzi, *et al.*, 2013). It is pointed out that zeolites and nanozeolites have utilized for zeolite modified electrodes (ZMEs) and applied in electrocatalysis reaction (Walcarius, 1999). Nickel is a relatively abundant and low cost material that is widely utilized in industrial applications. It is well understood that nickel can be used as an active catalyst due to its surface oxidation properties and has long-term stability in alkaline solutions (Raoof, *et al.*, 2011). Conversion of alcohols to carboxylic acids using a nickel electrode was described by Fleischmann (Fleischmann, *et al.*, 1971). Thereafter, nickel is widely applied for enhancement of electrode performance towards electrooxidation of HCHO (Raoof, *et al.*, 2012, Raoof, *et al.*, 2009, Enyo, 1986, Samadi-Maybodi, *et al.*, 2013, Fleischmann, *et al.*, 1971).

This study is an attempt to present a new, low cost and efficient catalyst for electrocatalytic oxidation of HCHO. Firstly, organic template-free hydrothermal synthesis of Ni-ZSM-5 and ZSM-5 nanozeolites has been performed and characterized. Then, these novel nanozeolites were used for modification of carbon paste electrode (CPE) and applied for electrocatalyticoxidation of HCHO in the alkaline medium by using cyclic voltammetry technique.

MATERIALS AND METHODS

Reagents and materials

HCHO, Tetraethylorthosilicat (TEOS), sodium aluminate, sodium hydroxide, potassium chloride, potassium hexacyanoferrate and $NiCl_2.6H_2O$ were of analytical reagent grade and were prepared from Merck Company and were used without any purification. Graphite powder and paraffin oil (density 0.88 gcm^{-3}) as the binding agent (both from Dayjung company) were used for preparing the pastes. Also double distilled water was used throughout.

Preparation of Ni-ZSM-5 nanozeolite

Ni-ZSM-5 nanozeolite has been synthesized using sodium aluminate ($NaAlO_2$) and tetraethylorthosilicat (TEOS) as aluminum and silica sources, respectively. In a typical synthesis, sodium aluminate was dissolved in sodium hydroxide solution under stirring, followed by successive addition of double distilled water and $NiCl_2.6H_2O$. Then, TEOS was added to the solution-and stirred until a homogeneous gel was obtained. The prepared gel was transferred in a Teflon lined stainless steel reactor and heated at 180°C for 24 h. The fabricated nanocrystals were centrifuged, washed several times with distilled water to remove impurity and dried at 90°C overnight. The molar ratio of the above reactants was as follows: 0.5 Al_2O_3: 0.5 NiO: 30 SiO_2: 3.3 Na_2O: 1350 H_2O. Also, ZSM-5 nanozeolite was prepared by a similar technique without $NiCl_2$ and the mole ratio of Al_2O_3 in the batch composition was 1.0.

Apparatus

XRD pattern was prepared by X-ray diffractometer

(XRD, GBC−MMA) with Be Filtered Cu Kα radiation (1.5418 Å) operating at 35.4 kV and 28 mA. The 2θ scanning range was set between 5º and 50º with scan rate of 0.05 degree/second. Scanning electron microscopy (SEM, VEGA2−TESCAN) was used to study morphology and size of fabricated crystal. Bruker FT-IR spectrometer (Vector 22) was employed for recording the fourier transform infrared (FT-IR) spectrum at ambient temperature. Energy-dispersive X-ray spectroscopy (EDX) spectra were recorded on an EDX Genesis XM2 attached to SEM. The electrochemical experiments were performed at ambient temperature by using potentiostat/galvanostat electrochemical analyzer (Ivium, Netherlands, V11100) with a voltammetry cell in a three electrodes configuration. The Ag|AgCl|KCl (3 M) and platinum wire were used as reference and auxiliary electrodes, respectively. The CPE, and modified carbon paste electrodes with ZSM-5 and Ni-ZSM-5 nanozeolites were used as working electrodes.

Preparation of working electrode

A suitable amount of Ni-ZSM-5 nanozeolite (5–30% wt with respect to graphite) was mixed with 200 mg of graphite powder to prepare Ni-ZSM-5/CPE and then paraffin oil (35% wt) was blended with the prepared mixture in a mortar by well hand mixing for 30 min until a homogeneously wetted paste was obtained. This ready paste was filled into the end of a glass tube (ca. 0.35 cm i.d. and 10 cm long). Copper wire was selected for electrical contact in prepared electrode. By pushing an excess of the paste out of the tube and polishing with a weighing paper, a new surface was obtained. For comparison, unmodified CPE and modified ZSM-5/CPE was also fabricated in the same way.

RESULTS AND DISCUSSION

Characterization of ZSM-5 nanozeolite

Fig. 1 shows XRD powder pattern with SEM image of Ni-ZSM-5 nanozeolite. Comparison of the main peaks at 2θ = 7.9, 8.9, 23.2 and 24.5 degrees with the reference sample (Gurses, *et al.*, 2006, Nejad-Darzi, *et al.*, 2013) indicated that pure phase of Ni-ZSM-5 nanozeolite was fabricated in this research. It is clear that when TEOS is applied as source of silicon in the gel composition, it can play as structure directing agent (SDA) in system and it can effect on the formation of Ni-ZSM-5 nanozeolite due to its hydrolyzation and production of alcohol (Zhang, *et al.*, 2012).

The SEM image of crystalline phase provides useful approach to determination of size and morphology of the prepared crystals. Inset in Fig.1 illustrates SEM image of synthesized Ni-ZSM-5 nanozeolite, which indicates the formation of spherical nano-sized parti-

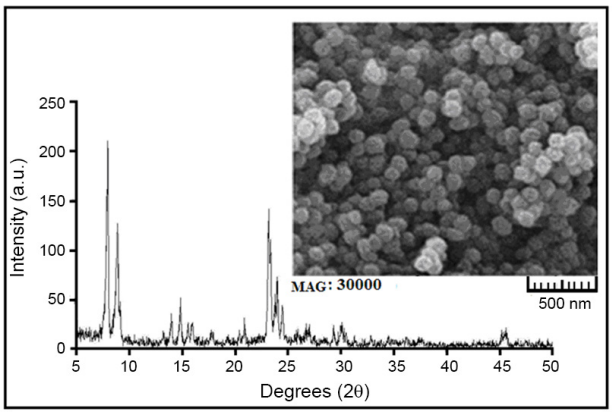

Fig. 1: The XRD pattern of Ni-ZSM-5 nanozeolite.Inset shows SEM image of this sample.

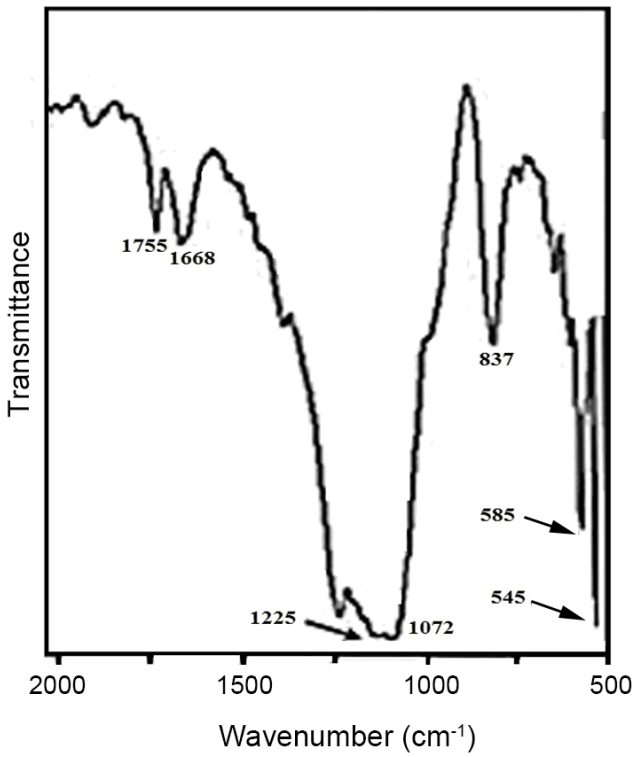

Fig. 2: The FT-IR spectrum of synthesized Ni-ZSM-5 nanozeolite.

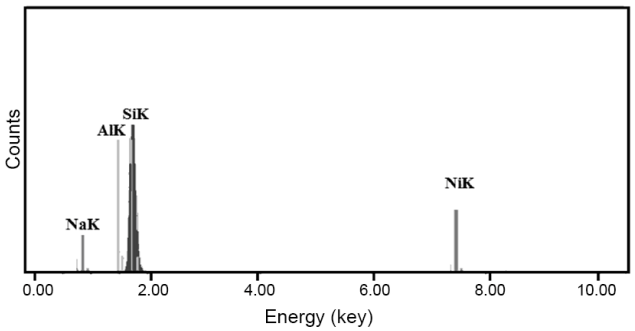

Fig. 3: The EDX spectrum of synthesized Ni-ZSM-5 nanozeolite.

cle. The average size of nanoparticle is around 85 nm. FT-IR spectrum of as-synthesized Ni-ZSM-5 nanozeolite is presented in Fig. 2. The bands located at 1070-1250 cm^{-1} are related of SiO_4 tetrahedron units. Difference between Ni-ZSM-5 nanozeolite and other types of zeolites can be found by the absorption bands at 1225 and 545 cm^{-1}. The external asymmetric stretching vibration near absorption bands at 1225 cm^{-1} is due to the presence of structures containing four chains of four-member rings between SiO_4 or AlO_4 tetrahedral of Ni-ZSM-5 structure and is a structure sensitive IR band of ZSM-5 zeolite (Mohamed, *et al.*, 2005, Abrishamkar, *et al.*, 2011). The bands near absorption bands at 1072 cm^{-1} and 837 cm^{-1} are assigned to the internal asymmetric stretching and external symmetric stretching of external linkages, respectively. Also, the absorption band about 545 cm^{-1} is attributed to a structure-sensitive vibration caused by the double four-member rings of the external linkages (Li and Armor, 1992).

The EDX spectroscopy analysis was also provided. This technique provides useful information about the presence of elements and their composition in the synthesized nanozeolites. Fig. 3 represents the EDX spectrum of Ni-ZSM-5 nanozeolite. Extracted data from this Fig. are listed in Table 1. The obtained data in Fig. 3 and Table 1 demonstrated that silicon, aluminum, nickel and sodium are presented in the synthesized Ni-ZSM-5 nanozeolite.

Table 1: Amounts of elements in Ni-ZSM-5 obtained by EDX analysis.

Element	NaK	AlK	SiK	NiK
Wt. %	7.45	12.32	67.43	12.80

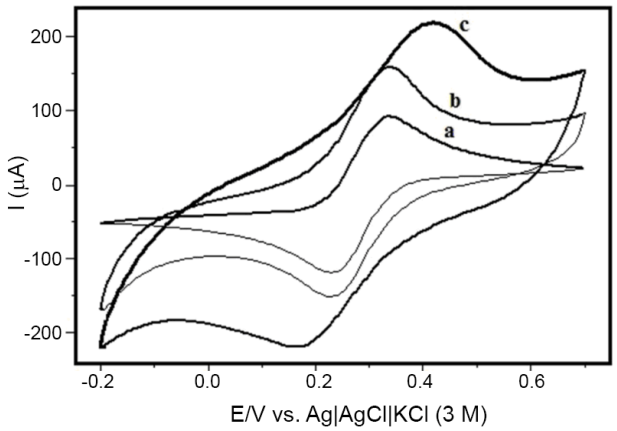

Fig. 4: CVs of (a) bare CPE, (b)ZSM-5/CPE and (c) Ni-ZSM-5/CPE in a solution of 10 mM $K_3Fe(CN)_6$]/ $K_4[Fe(CN)_6]$ (1:1) + 2 M KCl at a scan rate of 25 mV s^{-1}.

Electrochemistry of the modified electrode

Potassium ferricyanide was nominated as a probe to evaluate the performance of the fabricated electrodes. Also, cyclic voltammetry technique was employed for detection of electrochemical properties of the unmodified CPE, modified ZSM-5/CPE and Ni-ZSM-5/CPE electrodes. Fig. 4 represents the CVs of $Fe(CN)_6^{3-/4-}$ at the surface of three electrodes in 10 mM of $K_3Fe(CN)_6$/ $K_4Fe(CN)_6$ + 2 M of KCl solution. As can be seen in Fig. 4, the anodic peak current for Ni-ZSM-5/CPE is much larger than that ZSM-5/CPE and bare CPE. The anodic peak current was obtained to be 217, 159, 92 μA for Ni-ZSM-5/CPE, ZSM-5/CPE and bare CPE, respectively. The experimental results at slow

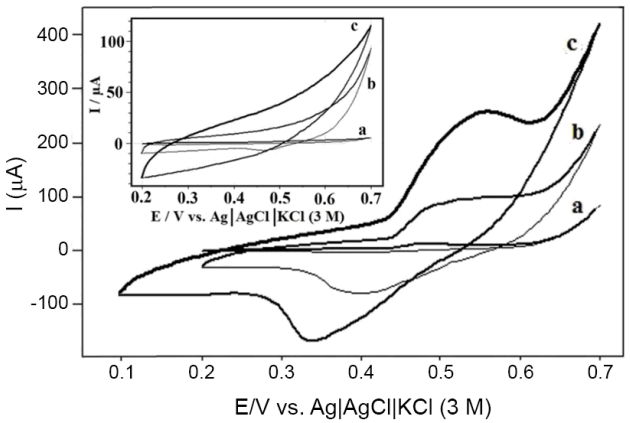

Fig. 5: CVs of (a) bare CPE, (b) ZSM-5/CPE and (c) Ni-ZSM-5/CPE at 0.1 M NaOH after immersed in 0.1 M $NiCl_2$ solution. Inset shows CVs of bare CPE, ZSM-5/CPE and Ni-ZSM-5/CPE at 0.1 M NaOH before immersed in 0.1 M $NiCl_2$ solution, the scan rate is 25 mV s^{-1}.

scan rates of 25 mVs^{-1} at the surface of Ni-ZSM-5/CPE showed reproducible cathodicand anodic peaks related to $Fe(CN)_6^{3-}/Fe(CN)_6^{4-}$ redox couple with quasi-reversible behavior with a peak separation potential, $\Delta E_p(E_{pa} - E_{pc})$, of 255 mV. The ΔE_p is greater than that of 59 mV expected for a reversible system. It can be noted that the electrochemical properties of the $Fe(CN)_6^{3-}/Fe(CN)_6^{4-}$ redox couple in the Ni-ZSM-5/CPE electrode surface are pH independent.

Electrochemical behavior of Ni-ZSM-5/CPE in alkaline solution

Inset in Fig. 5 shows CVs of bare CPE, ZSM-5/CPE and Ni-ZSM-5/CPE in 0.1 M NaOH solution at the potential range between 0.2 to 0.7 V vs. Ag|AgCl|KCl (3 M) at scan rate of 20 mV s^{-1}. The obtained results showed that no current can be obtained with these electrodes and the background current for Ni-ZSM-5/CPE is much larger than that on bare CPE andZSM-5/CPE because the surface area is bigger than two others (Safavi, *et al.*, 2009).

In the next experiment, three fabricated electrodes (bare CPE, ZSM-5/CPE and Ni-ZSM-5/CPE) were immersed in the 0.1 M $NiCl_2$ solution with stirring for five minutes at 150 rpm, and then each three electrodes washed completely with distilled water to remove the surface adsorbed species. The main panel of Fig. 5 illustrates CVs of these electrodes in 0.1 M NaOH solution after immersion of these electrodes in 0.1 M $NiCl_2$ solution at a potential sweep rate of 20 mV s^{-1}. It can be deduced that the electrochemical behavior of Ni-ZSM-5/CPE modified electrode in alkaline solution is similar to that of Ni anode (Fleischmann, *et al.*, 1971, Nagashree and Ahmed, 2010). A probable mechanism is that at Ni-ZSM-5 nanozeolite/electrolyte interface, Ni^{2+} ions react with OH^- ions to create nickel hydroxide ($Ni(OH)_2$). During the anodic direction, the $Ni(OH)_2$ at the surface of Ni-ZSM-5/CPE is converted to the nickel oxy-hydroxide (NiOOH) and in cathodic direction NiOOH is reduced to $Ni(OH)_2$ based on the following reaction (Nagashree and Ahmed, 2010, Fleischmann, *et al.*, 1971, Samadi-Maybodi, *et al.*, 2013):

$$\left[(Ni-ZSM-5/CPE)-Ni(OH)_2\right]+OH^- \leftrightarrow \left[(Ni-ZSM-5/CPE)-NiOOH\right] + H_2O + e^- \quad (1)$$

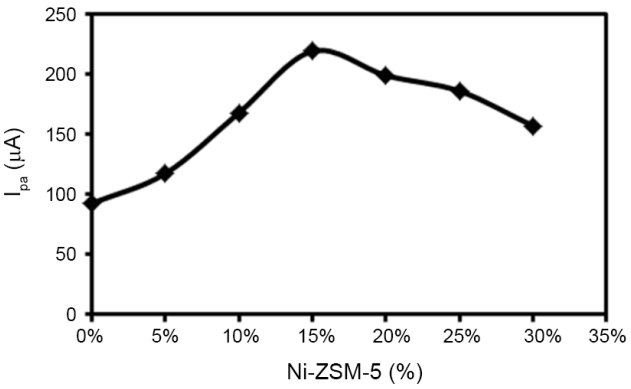

Fig. 6: Variation of anodic peak current with Ni-ZSM-5 percentage in preparation of modified electrodes.

A pair of redox peaks appears at 0.560 and 0.335 V vs. Ag|AgCl|KCl (3 M) is assigned to Ni^{2+}/Ni^{3+} redox couple. As can be seen in Fig. 5, the peak current of $Ni(OH)_2$ oxidation at the surface of Ni-ZSM-5/CPE is 2.65-fold greater than that at the ZSM-5/CPE and is about 25.5-fold greater than that at the bare CPE. These observations can explain clearly the role of the Ni-ZSM-5 nanozeolite on the enhancement of the oxidation currents. The separation of anodic and cathodic peak of $Ni(OH)_2$ to NiOOH and reversed conversion is obtained to be 225 mV (i.e. 0.560 and 0.335 mV for anodic and cathodic peaks, respectively) for Ni-ZSM-5/CPE modified electrode (see Fig.5c). It can be realized that this phenomena is a quasi-reversible procedure because the ΔE_p is greater than that of 59/n mV expected for a reversible system. The peak-to-peak potential separation is deviated from the theoretical value of zero and increased at higher potential sweep rates. The variation between the voltammetric behaviors of Ni^{2+} ions in Ni-ZSM-5/CPE, ZSM-5/CPE and bare CPE electrodes appeared to be due to the different coordination and mobility of Ni^{2+} ions in various site of CPE, ZSM-5 and Ni-ZSM-5 nanozeolites. It can be expected that diffusion of Ni^{2+} ions in Ni-ZSM-5 nanozeolite is much faster owing to their coordination to the nanozeolitestructure, the bigger cages and channels and fast migration of Ni^{2+} ions from the cages (Li and Calzaferri, 1994). These results are in excellent agreement with earlier observations (Ojani, *et al.*, 2008, Mojovic, *et al.*, 2007, Fleischmann, *et al.*, 1971, Samadi-Maybodi, *et al.*, 2013) although the exact potential values may change due to experimental conditions.

Voltammetric responses of the modified electrodes with Ni-ZSM-5 nanozeolite ratio of 5, 10, 15, 20, 25 and 30% (w/w) with respect to the graphite powder were studied by CV technique at 0.1 M of NaOH solution. The CVs of $Ni(OH)_2$/NiOOH oxidation on different modified electrodes showed that higher anodic current is obtained in 15% of Ni-ZSM-5 nanozeolite-with respect to the graphite powder (see Fig.6). It is recommended that at low ratio of Ni-ZSM-5 nanozeolite, the amount of nanozeolite is so low in the modified electrodes that the available pores for Ni^{2+} insertion can be decreased. Also, with increasing the Ni-ZSM-5 nanozeolite over 15% in the modified electrodes, the resistance of the electrode increased leading to a decrease in anodic current and sensitivity of the electrode response (Samadi-Maybodi, *et al.*, 2013, Raoof, *et al.*, 2011, Azizi, *et al.*, 2013).

Effect of different scan rates on modified fabricated electrode was investigated. Fig.7A illustrates the CVs of the Ni-ZSM-5/CPE electrode in 0.1 M NaOH at different scan rates. Obviously, the height of the anodic current enhanced with increasing of scan rate and potential also moved to positive values. This positive shift may be due to the ohmic drop which generated at high current density. The ΔE_p increased with scan rate that indicated a limitation in charge transfer kinetics due to the chemical interactions between the electrolyte ions and the modified electrode. For $\Delta E_p > 200/n$ mV, ordinarily obtained at higher scan rates, the following relations existed for the linear potential sweep voltammetric response proposed by Laviron (Laviron, 1979).

$$E_{pa} = E^0 + X\ln\left[\frac{1-\alpha}{nF}\right] \quad (2)$$

$$E_{pc} = E^0 + Y\ln\left[\frac{\alpha}{m}\right] \quad (3)$$

where $X = RT/(1-\alpha)nF$, $m = (RT/F)(ks/nv)$, $Y = RT/\alpha n F$, E_{pa} and E_{pc} are the anodic and cathodic peak potentials, respectively. Also, α, k_s, and $\upsilon$are the electron-transfer coefficient, apparent charge-transfer rate constant and scan rate, respectively. From these expressions, the α can be determined by measuring the

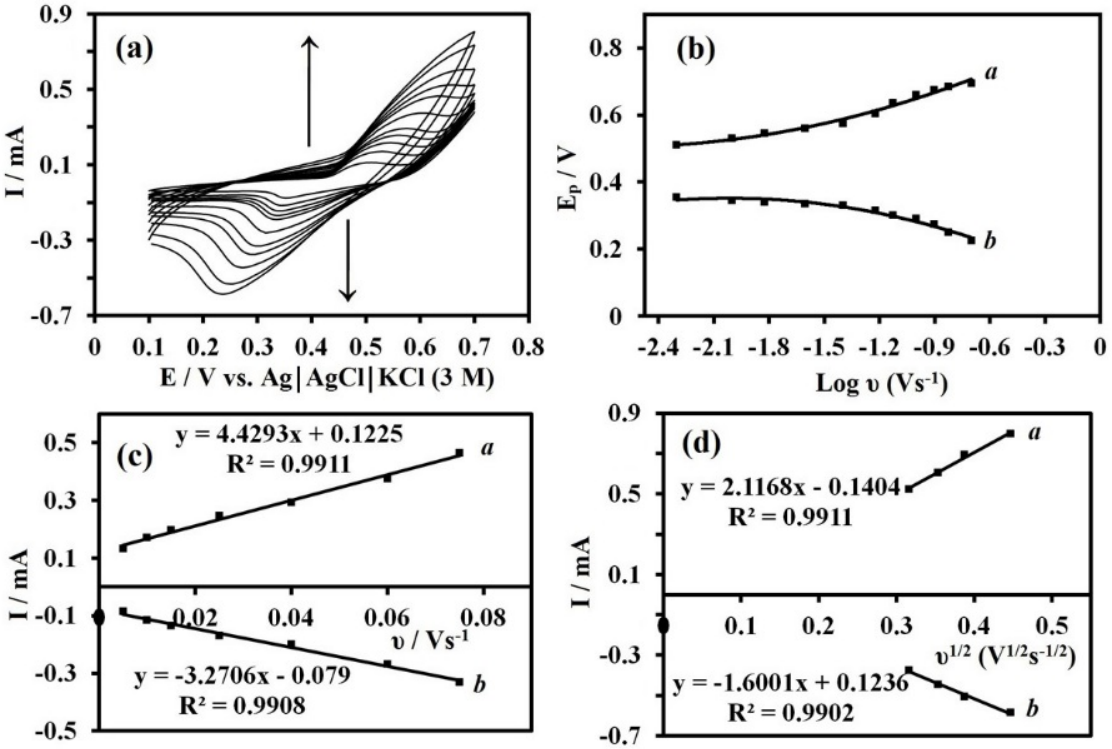

Fig. 7: (a) CVs of the Ni-ZSM-5/CPE in 0.1 M NaOH at various scan rates from inner to outer: 0.005, 0.010, 0.015, 0.025, 0.040, 0.060, 0.075, 0.100, 0.125, 0.150 and 0.200 V s^{-1}. (b) Plot of E_p vs. log υ for CVs showed in the (a) for anodic peaks (a) and cathodic peaks (b). (c) The dependency of I_{pa} (a) and I_{pc} (b) on lower values of υ (0.01–0.075 V s^{-1}) and (d) Plot of I_{pa} (a) and I_{pc} (b) on $\upsilon^{1/2}$ at higher values of υ (υ> 0.075 V s^{-1}).

variation of the peak potential with respect to the scan rate, and ks can be determined for electron transfer between the electrode and the surface-deposited layer by measuring the E_p values.

Fig. 7B displays the plot of E_p with respect to the logarithm of scan rate from CVs at the ranges of 0.005–0.20 V s^{-1} for both anodic and cathodic peaks. It can be seen that E_p is proportional to log υ at υ> 0.075 V s^{-1} proven by Laviron (Laviron, 1979). The value of anodic electron transfer coefficient (α) is obtained 0.49. These values suggest that the activation energy for the reduction and oxidation processes might be the same (Luo, *et al.*, 2001, Zheng, *et al.*, 2009). The mean value of charge-transfer rate constant (k_s) is found to be 0.045 s^{-1}.

Fig. 7C illustrates plots of anodic and cathodic peak currents for oxidation–reduction of the NiOOH/$Ni(OH)_2$ redox couple versus scan rate at low values from 0.01 to 0.075 V s^{-1}. This dependence is probably due to electrochemical activity of immobilized redox species at the surface of modified electrode. The electrode surface coverage (Γ*) can be calculated from linear section of the plot and using the following equation which correspond to reversible process with adsorbed species (Bard and Faulkner, 2006).

$$I_p = \frac{n^2F^2A\Gamma^*\upsilon}{4\ R\ T} \quad (4)$$

Where I_p, n, A and Γ* be the peak current, the number of electrons involved in the reaction (n=1), the surface area of the electrode (0.0962 cm^2) and the surface coverage of the redox species, respectively. From plot of anodic current vs. scan rate and the above equation, the total surface coverage of the Ni-ZSM-5/CPE was calculated to be 4.11×10^{-8} mol cm^{-2}, considering the mean of both anodic and cathodic currents.

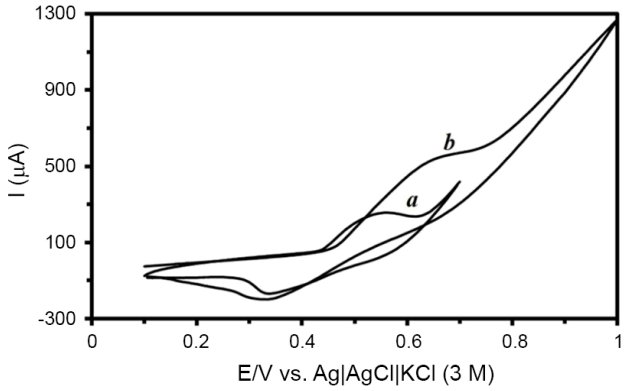

Fig. 8: CVs of Ni-ZSM-5/CPE in the (a) absence and (b) presence of 0.010 M HCHO in 0.1 M NaOH at scan rate of 20 mV s^{-1}.

Fig. 7D shows plots of anodic and cathodic peak currents vs.$\upsilon^{1/2}$ at υ>0.075 V s^{-1}. It can be concluded that the charge-transport through the Ni-ZSM-5/CPE modified electrode is controlled by diffusion. This limiting-diffusion process may be due to the charge neutralization of the electrode surface during the oxidation/reduction process (Taraszewska and Rosłonek, 1994, Azizi, *et al.*, 2013).

Electrocatalytic oxidation of HCHO at the surface of Ni-ZSM-5/CPE

The electrochemical oxidation of HCHO at the surface of Ni-ZSM-5/CPE was investigated in 0.1 M NaOH solution.The electrochemical response of the Ni-ZSM-5/CPE in 0.1 M NaOH solution exhibited well-defined cathodicand anodic peaks associated with Ni(III)/Ni(II) redox couple (see Fig. 8a).

Fig. 8b demonstrates the CV for electrocatalytic oxidation of the HCHOon the surface of Ni-ZSM-5/CPE in 0.01 M HCHO + 0.1 M NaOH at scan rate of 20 mV s^{-1}. Addition of HCHO to the electrolyte solution caused an enhancement in the anodic peak current. Comparison of curves (a) and (b) in Fig. 8 demonstrated that utilization of Ni-ZSM-5 as incorporated materials into a carbon paste electrode improved the electrochemical signal of HCHO oxidation. The $Ni(OH)_2$ layer at the electrode surface can act as a catalyst for oxidation of HCHO. As can be seen in this Fig., the pair of peaks around0.560 and 0.335 V that seen in Fig. 8a (corresponding to the NiOOH/$Ni(OH)_2$ conversion) were vanished in the presence of HCHO, meanwhile a new oxidation peak appeared around 0.71 V. A comparison between the CVs of Ni-ZSM-5/CPE modified electrode in 0.1 M NaOH solution in the absence (Fig. 8a) and presence (Fig. 8b) of HCHO specified that anodic current for HCHO oxidation is 575 μA, meanwhile anodic current is 256 μA for $Ni(OH)_2$/NiOOH conversion in the same scan rate (i. e. 20 mV s^{-1}). It can be concluded that the applied modifier in this process contributed directly to the electrocatalytic oxidation of HCHO with EC′ mechanism.

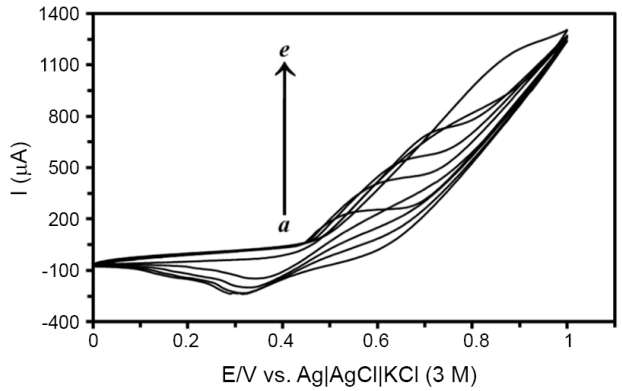

Fig. 9: Current-potential curves of different HCHO concentrations: (a) 0.0, (b) 3.0, (c) 10.0, (d) 25.0 and (e) 50.0 mM at the Ni-ZSM-5/CPE and scan rate of 20 mV s^{-1}.

HCHO molecule is almost hydrated and converted to the methylene glycol ($CH_2(OH)_2$) (Koper, *et al.*, 1996). Due to its pKa of ca. 12.8, the $CH_2(OH)_2$ exists predominantly in its ionized form ($CH_2(OH)O^-$) in 0.1 M NaOH solution. When $CH_2(OH)O^-$ diffuses from the bulk mediaon surface of electrode and is quickly oxidized to $CH_2(O)O^-$ by the NiOOH species on the electrode surface that generated according equation 1. Hence, the amount of NiOOH species decreases due to its chemical reaction with HCHO. Mechanism of HCHO oxidation at the surface of Ni-ZSM-5/CPE can be described by the following equation (Yang, *et al.*, 1999, Raoof, *et al.*, 2012, Ciszewski and Milczarek, 1999, Zhao, *et al.*, 2006):

$$\left[(\text{Ni}-\text{ZSM}-5/\text{CPE})-\text{NiOOH}\right]+\text{HCHO}\leftrightarrow \text{Products} +\left[(\text{Ni}-\text{ZSM}-5/\text{CPE})-\text{Ni(OH)}_2\right] \quad (5)$$

Effect of HCHO concentration

Fig. 9 illustrates the effect of HCHO concentration on its electrooxidation current onto Ni-ZSM-5/CPE at scan rate of 20 mV s^{-1}. It is clearly observed that the anodic peak current increased with increasing of HCHO up to the concentration of 50.0 mM. In the concentrations above 50.0 mM, no remarkable increase in the anodic peak current was observed (data not shown). It can be stated that this effect may be due to the saturation of active sites and/or poisoning the electrode surface with adsorbed intermediates. Thus, 50.0 mM of HCHO represented the optimumconcentration after which the adsorption of the oxidation products at the electrode surface may cause the stoppage of further oxidation.

The effect of scan rate on the electrocatalytic oxidation of HCHO (0.01 M) was also studied. The peak currents (I_p) increased and the anodic peak potentials shifted to more positive directions by an increase in the scan rate (data not shown). It can be regarded to a kinetic limitation in the reaction between the redox sites of the HCHO and Ni-ZSM-5/CPE. Moreover, linear dependency of anodic peak currents versus the square root of the scan rate ($\upsilon^{1/2}$) indicated that the electrode reaction is a diffusion controlled process.

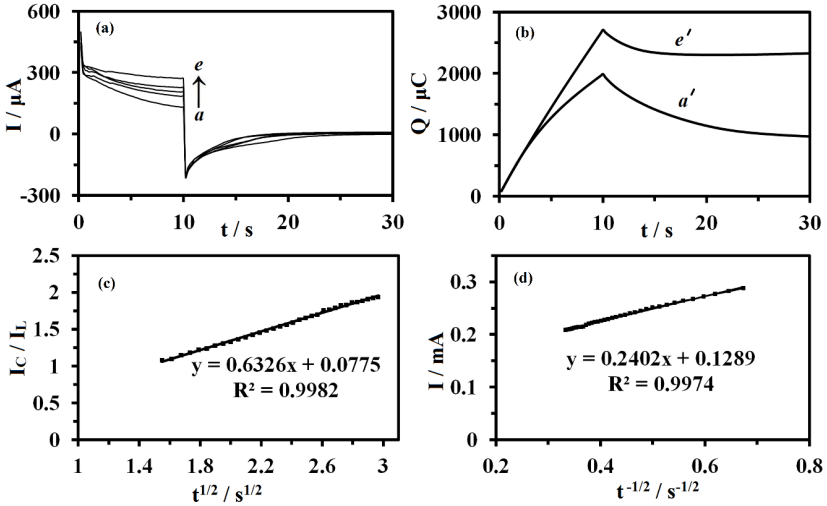

Fig. 10: :(a) Double step chronoamperograms of Ni-ZSM-5/CPE in 0.1 M NaOH solution in the absence (a) and presence of (b) 0.003, (c) 0.005, (d) 0.01 and (e) 0.03 M of HCHO. The potential steps were 0.730 and 0.350 V vs. Ag/AgCl/ KCl (3 M). (b) Charge-time curves in the absence (a') and presence of 0.03 M of HCHO (e'). (c) Dependence of IC/IL on t1/2, derived from the data of chronoamperograms (a) and (e). (d) Dependence of I on $t^{-1/2}$, derived from the data of chronoamperogram (c).

Chronoamperometric studies

The electrocatalytic oxidation of HCHO at the surface of modified electrode was also studied using chronoamperometry method. Fig. 10A shows double step chronoamperometric measurements at the surface of the Ni-ZSM-5/CPE at different concentrations of HCHO such as 0.00, 0.003, 0.005, 0.01 and 0.03 M. The applied potential steps were 0.73 and 0.35 V vs. Ag|AgCl|KCl (3 M) in the anodic and cathodic direction, respectively.The forward and backward potential step chronoamperometry of the Ni-ZSM-5/CPE electrode in the blank solution showed an almost symmetrical chronoamperogram, which shows that almost equivalent charges were consumed for the oxidation and reduction of surface confined $Ni(OH)_2$/NiOOH sites. However, in the presence of HCHO, the charge value (Q) associated with the forward chronoamperometry is greater than that observed for the backward chronoamperometry (see Fig. 10B).

Chronoamperometry can be applied for the approximation of the catalytic rate constant (k) between the HCHO and redox sites of electrode based on equation (7) (Bard and Faulkner, 1980):

$$\frac{I_C}{I_L} = \gamma^{1/2}\left[\pi^{1/2}\mathrm{erf}(\gamma)^{1/2} + \frac{\exp(-\gamma)}{\gamma^{1/2}}\right] \quad (6)$$

where, IC and IL are the currents in the presence and absence of HCHO, respectively. Symbol $\gamma = kc_0t$ is the argument of error function, k is the catalytic rate constant ($cm^3mol^{-1}\ s^{-1}$), c_0 is the bulk concentration of HCHO ($molcm^{-3}$) and t is the elapsed time (s). When γ exceeds 1.5, erf ($\gamma^{1/2}$) is nearly equal to 1 and the above equation can be summarized to:

$$\frac{I_C}{I_L} = \gamma^{1/2}\pi^{1/2} = \pi^{1/2}(kc_0t)^{1/2} \quad (7)$$

Fig. 10C shows plot of I_C/I_L versus $t^{1/2}$ derived from the data of chronoamperograms in the absence of HCHO (a) and in the presence of 0.03 M HCHO (e). From the slopes of the I_C/I_L versus $t^{1/2}$ for all concentrations, the mean value of k was found to be 9.064×10^3 $cm^3mol^{-1}\ s^{-1}$. An exponential behavior of I–t curves shows that a diffusion-controlled process has occurred according to Cottrell equation (Bard and Faulkner, 1980). From the chronoamperometric study, the diffusion coefficient, D, of HCHO was determined in aqueous solution by the following equation (Hassaninejad-Darzi and Ra-

Table 2: Comparison of the electrocatalytic behavior of Ni-ZSM-5/CPE for oxidation of formaldehyde with some of the previously reported electrodes.

Electrode	Electrolyte	Saturation limit of HCHO for current (mol cm^{-3})	Scan rate (mV s^{-1})	E_p/V vs. (Ag/AgCl)	Current density (mA cm^{-2})	Ref.
Cu/P(2ADPA)/MCNTPE	0.2 M NaOH	0.17	20	0.63	25.56	1
Pt/SWCNT/PANI	0.5 M $HClO_4$	0.50	50	0.66	90.0	8
Pt/PAANI/MWNTs/GCE	0.5 M H_2SO_4	0.50	50	0.45	7.32	10
Pt/Carbon-Ceramic	0.1 M H_2SO_4	0.75	20	0.85	31.40	11
Pd–CILE	0.1 M NaOH	0.30	100	0.15	9.40	20
Ni/P(1,5-DAN)/MCPE	0.1 M NaOH	0.17	10	0.80	0.76	27
$Ni(OH)_2$/POT (TX-100)/MCNTPE	0.1 M NaOH	0.048	20	0.70	12.70	29
Ni/P(NMA)/MCPE	0.1 M NaOH	0.07	20	0.74	4.10	30
Ni-ZSM-5/CPE	0.1 M NaOH	0.050	20	0.71	13.02	This work

himnejad, 2014, Bard and Faulkner, 1980):

$$I = nFACD^{1/2}.\pi^{-1/2}.t^{-1/2} \quad (8)$$

Where F is the faraday number, A is the area of the electrode, C is the known concentration of compound and D is the apparent diffusion coefficient. Fig. 10D demonstrates experimental plots of I vs. $t^{-1/2}$ for 0.005 M of HCHO at the surface of Ni-ZSM-5/CPE. The same curves were plotted for all concentrations and then the slopes of the resulting straight lines were plotted vs. the HCHO concentration. From the slope of the resulting plots and using the Cottrell equation, the mean value of the D was achieved to be 8.575×10^{-6} cm^2 s^{-1} (with n=1, F=96485 C mol^{-1}, and A=0.0962 cm^2). A linear relationship in the plot I vs. $t^{-1/2}$ indicated that the electrode reaction is a diffusion controlled process and this result is in good agreement with cyclic voltammetric experiments (see previous section).

Stability of the Ni-ZSM-5/CPE

In the practical view, stability of the modified electrode was examined by measuring its response to HCHO oxidation after 1 and 3 months of storage in the laboratory atmosphere condition using CV technique. The electrode response to electrocatalyticoxidation of HCHO retains 94% and 86% of initial value, respectively. In comparison with some other previous works, it seems clearly that nickel hydroxide in the Ni-ZSM-5/CPE can act as a comparable catalyst in the oxidation of HCHO. Table 2 exhibits peak potential, peak current density and saturation limit of HCHO for current of the Ni-ZSM-5/CPE modified electrode toward the electrooxidation of HCHO in 0.1 M NaOH with some modified electrode reported in the literature. In comparison with some previous reported works, it seems that Ni-ZSM-5/CPE can act as an efficient electrocatalyst in HCHO oxidation process. It can be noted that the comparison of the efficiency in terms of anodic peak potential and stability for HCHO oxidation at low cost modified electrode (E_p= 0.71 V) shows that this value is less than that previous works and comparable with the precious metal (i.e., Pt, Pd and Cu) modified electrodes. Besides, the surface modification of the electrode is very simple and reproducible compared to other modified electrodes.

CONCLUSIONS

In this done research,an organic template-free method was developed to the synthesis of Ni-ZSM-5 and ZSM-5 nanozeolites. Then, a novel modified CPEs were prepared by Ni-ZSM-5 and ZSM-5 nanozeolites. The electrocatalytic oxidation of HCHO onthe surface of Ni-ZSM-5/CPE was investigated by using of CV techniques. The Ni-ZSM-5/CPE modified electrode had large electrochemical surface area, and exhibited the superior electrocatalytic performance foroxidation of HCHO with decreasing over potential versus bare CPE and ZSM-5/CPE and showed good electrocatalytic activity toward HCHO compared to many of the previously reported electrodes. Results revealed that the NiOOH species formed during the oxidation of Ni-ZSM-5/CPE is found to be a good catalyst for oxidation of HCHOand the modified electrode can overcome the kinetic limitation by a catalytic process. However, this non-noble catalyst has some advantages such as low cost and stability, ease of preparation and regeneration, stable response and very low ohmic resistance in fuel cell.

REFERENCES

Ojani, R.; Raoof, J.B.; Ahmady-Khanghah, Y.; Safshekan, S.; (2013). Copper-poly (2-aminodiphenylamine) composite as catalyst for electrocatalytic oxidation of formaldehyde. Int. J. Hydrogen Energy, 38: 5457-5463.

Mai, C.F.; Shue, C.H.; Yang, Y.C.; Ou Yang, L.Y.; Yau, S.L.; Itaya, K.; (2005). Adsorption of formaldehyde on Pt (111) and pt (100) electrodes: Cyclic voltammetry and scanning tunneling microscopy. Langmuir, 21: 4964.

Samjeske, G.; Miki, A.; Osawa, M.; (2007). Electrocatalytic oxidation of formaldehyde on platinum under galvanostatic and potential sweep conditions studied by time-resolved surface-enhanced infrared spectroscopy. J. Phys. Chem. C, 111: 15074–15083.

Santos, M.; Bulhoes, L.; (2004). Electrogravimetric investigation of formaldehyde oxidation at Pt electrodes in acidic media. Electrochim. Acta, 49:

1893–1901.

Korzeniewski, C.; Childers, C.L.; (1998). Formaldehyde yields from methanol electrochemical oxidation on platinum. J. Phys. Chem. B, 102: 489–492.

Miki, A.; Ye, S.; Senzaki, T.; Osawa, M.; (2004). Surface-enhanced infrared study of catalytic electrooxidation of formaldehyde, methyl formate, and dimethoxymethane on platinum electrodes in acidic solution. J. Electroanal. Chem., 563: 23–31.

Lima, R.D.; Massafera, M.; Batista, E.; Iwasita, T.; (2007). Catalysis of formaldehyde oxidation by electrodeposits of PtRu. J. Electroanal. Chem., 603: 142–148.

Wang, Z.; Zhu, Z.-Z.; Shi, J.; Li, H.-L.; (2007). Electrocatalytic oxidation of formaldehyde on platinum well-dispersed into single-wall carbon nanotube/polyaniline composite Film. Appl. Sur. Sci., 253: 8811–8817.

Wang, D.; Wang, J.; Lu, S.; Jiang, S.P.; (2014).Facile synthesis of sub-monolayer Sn, Ru, and RuSn decorated Pt/C nanoparticles for formaldehyde electrooxidation. J.Electroanal. Chem., 712: 55–61.

Jiang, C.; Chen, H.; Yu, C.; Zhang, S.; Liu, B.; Kong, J.; (2009). Preparation of the Pt nanoparticles decorated poly (N-acetylaniline)/MWNTs nanocomposite and its electrocatalytic oxidation toward formaldehyde. Electrochim. Acta, 54: 1134–1140.

Habibi, B.; Delnavaz, N.; (2010). Electrocatalytic oxidation of formic acid and formaldehyde on platinum nanoparticles decorated carbon-ceramic substrate. Int. J. Hydrogen Energy, 35: 8831–8840.

Mascaro, L.H.; Goncalves, D.; Bulhoes, L.O.S.; (2004). Electrocatalytic properties and electrochemical stability of polyaniline and polyaniline modified with platinum nanoparticles in formaldehyde medium. Thin Solid Films, 461: 243–249.

Li, M.; Wang, W.; Ma, C.; Zhu, W.; (2011). Enhanced electrocatalytic activity of Pt nanoparticles modified with PPy-HEImTfa for electrooxidation of formaldehyde. J. Electroanal. Chem., 661: 317–321.

Ramanauskas, R.; Vaskelis, A.; (1997). Electrocatalytic oxidation of formaldehyde on copper single crystal electrodes in alkaline solutions. Electrochim. Acta, 42: 191–195.

Brunelli, K.; Dabala, M.; Magrini, M.; (2002). Cu-based amorphous alloy electrodes for fuel cells. J. Appl. Electrochem., 32: 145–148.

Vaskelis, A.; Tarozaite, R.; Jagminiene, A.; Tamasiunaite, L.T.; Juskenas, R.; Kurtinaitiene, M.; (2007). Gold nanoparticles obtained by Au (III) reduction with Sn (II): Preparation and electrocatalytic properties in oxidation of reducing agents. Electrochim. Acta, 53: 407–416.

Yahikozawa, K.; Nishimura, K.; Kumazawa, M.; Tateishi, N.; Takasu, Y.; Yasuda, K.; Matsuda, Y.; (1992). Electrocatalytic properties of ultrafine gold particles supported onto glassy carbon substrates toward formaldehyde oxidation in alkaline media. Electrochim. Acta, 37: 453–455.

Yang, H.; Lu, T.; Xue, K.; Sun, S.; Lu, G.; Chen, S.; (1999). Electrocatalytic mechanism for formaldehyde oxidation on the highly dispersed gold microparticles and the surface characteristics of the electrode. J. Mol. Catal. A-Chem., 144: 315–321.

Safavi, A.; Maleki, N.; Farjami, F.; Farjami, E.; (2009). Electrocatalytic oxidation of formaldehyde on palladium nanoparticles electrodeposited on carbon ionic liquid composite electrode. J.Electroanal. Chem., 626: 75–79.

Zhu, Z.-Z.; Wang, Z.; Li, H.-L.; (2009). Self-assembly of palladium nanoparticles on functional multi-walled carbon nanotubes for formaldehyde oxidation. J. Power Sources, 186: 339–343.

Gao, G.-Y.; Guo, D.-J.; Li, H.-L.; (2006). Electrocatalytic oxidation of formaldehyde on palladium nanoparticles supported on multi-walled carbon nanotubes. J. Power Sources, 162: 1094–1098.

Yi, Q.; Niu, F.; Yu, W.; (2011). Pd-modified TiO_2 electrode for electrochemical oxidation of hydrazine, formaldehyde and glucose. Thin Solid Films, 519: 3155–161.

Zhang, X.-G.; Murakami, Y.; Yahikozawa, K.; Takasu, Y.; (1997). Electrocatalytic oxidation of formaldehyde on ultrafine palladium particles supported on a glassy carbon. Electrochim. Acta, 42: 223–227.

Enyo, M.; (1985). Electrocatalysis by Pd+Au alloys Part II. Electro-oxidation of formaldehyde in acidic and alkaline solutions. J. Electroanal. Chem., 186: 155–166.

Abdel Aal, A.; Hassan, H.B.; Abdel Rahim, M.;

(2008). Nanostructured Ni–P–TiO_2 composite coatings for electrocatalytic oxidation of small organic molecules. J. Electroanal. Chem., 619: 17–25.

Ojani, R.; Raoof, J.-B.; Hosseini Zavvarmahalleh, S.R.; (2009). Preparation of Ni/poly (1, 5-diaminonaphthalene)-modified carbon paste electrode; application in electrocatalytic oxidation of formaldehyde for fuel cells. J. Solid State Electrochem., 13: 1605–1611.

Raoof, J.-B.; Azizi, N.; Ojani, R.; Ghodrati, S.; Abrishamkar, M.; Chekin F.; (2011). Synthesis of ZSM-5 zeolite: Electrochemical behavior of carbon paste electrode modified with Ni (II)–zeolite and its application for electrocatalytic oxidation of methanol. Int. J. Hydrogen Energy,36: 13295–13300.

Raoof, J.-B.; Ojani, R.; Abdi, S.; Hosseini, S.R.; (2012). Highly improved electrooxidation of formaldehyde on nickel/poly (o--toluidine)/Triton X-100 film modified carbon nanotube paste electrode. Int. J. Hydrogen Energy, 37: 2137–2146.

Raoof, J.-B.; Omrani, A.; Ojani, R.; Monfared, F.;(2009). Poly (N-methylaniline)/nickel modified carbon paste electrode as an efficient and cheep electrode for electrocatalytic oxidation of formaldehyde in alkaline medium. J. Electroanal. Chem., 633: 153–158.

Enyo, M.; (1986). Electrooxidation of formaldehyde on Cu+Ni alloy electrodes in alkaline solutions. J.Electroanal. Chem., 201: 47–59.

Samadi-Maybodi, A.; Hassani Nejad-Darzi, S.K.; Ganjali, M.R.; Ilkhani, H.; (2013). Application of nickel phosphate nanoparticles and VSB-5 in the modification of carbon paste electrode for electrocatalytic oxidation of methanol. J. Solid State Electrochem., 17: 2043–2048.

Hassani Nejad-Darzi, S.K.; Samadi-Maybodi, A.; Ghobakhluo, M.; (2013). Synthesis and characterization of modified ZSM-5 nanozeolite and their applications in adsorption of Acridine Orange dye from aqueous solution. J. Porous Mater., 20: 909–916.

Li, L.; Li, W.; Sun, C.; Li, L.; (2002). Fabrication of carbon paste electrode containing 1: 12 phosphomolybdic anions encapsulated in modified mesoporous molecular sieve MCM-41 and its electrochemistry. Electroanalysis, 14: 368–375.

Cundy, C.S.; Cox, P.A.; (2005). The hydrothermal synthesis of zeolites: precursors, intermediates and reaction mechanism. Micropor. Mesopor. Mater., 82: 1–78.

Song, J.; Dai, L.; Ji, Y.; Xiao, F.-S.;(2006). Organic template free synthesis of aluminosilicate zeolite ECR-1. Chem. Mater., 18: 2775–2777.

Zhang, L.; Liu, S.; Xie, S.; Xu, L.; (2012). Organic template-free synthesis of ZSM-5/ZSM-11 co-crystalline zeolite. Micropor. Mesopor. Mater., 147: 117–126.

Walcarius, A.; (1999). Zeolite-modified electrodes in electroanalytical chemistry. Anal. Chim. Acta, 384: 1–16.

Fleischmann, M.; Korinek, K.; Pletcher, D.; (1971). The oxidation of organic compounds at a nickel anode in alkaline solution. J. Electroanal. Chem., 31: 39–49.

Ciszewski, A.; Milczarek, G.; (1999). Kinetics of electrocatalytic oxidation of formaldehyde on a nickel porphyrin-based glassy carbon electrode. J. Electroanal. Chem., 469: 18–26.

Gurses, A.; Dogar, C.; Yalc, M.; Akyldz, M.; Bayrak, R.; Karaca, S.; (2006). The adsorption kinetics of the cationic dye, methylene blue, onto clay. J. Hazard. Mater., 131: 217–228.

Mohamed, R.M.; Aly, H.M.; El-Shahat, M.F.; Ibrahim, I.A.; (2005). Effect of the silica sources on the crystallinity of nanosized ZSM-5 zeolite. Micropor.Mesopor. Mater.,79: 7–12.

Abrishamkar, M.;Azizi, S.N.; Kazemian, H.; (2011). Using taguchi robust design method to develop an optimized synthesis procedure for nanocrystals of ZSM-5 zeolite. Z.Anorg.Allg. Chem., 637: 154–159.

Li, Y.; Armor, J.; (1992). Catalytic reduction of nitrogen oxides with methane in the presence of excess oxygen. Appl. Catal. B,1: L31–L40.

Nagashree, K.; Ahmed, M.; (2010). Electrocatalytic oxidation of methanol on Ni modified polyaniline electrode in alkaline medium. J. Solid State Electrochem., 14: 2307–2320.

Li, J.-W.; Calzaferri, G.; (1994). Copper-zeolite-modified electrodes: An intrazeolite ion transport

mechanism. J. Electroanal. Chem., 377: 163–175.

Ojani, R.; Raoof, J.-B.; Hosseini Zavvarmahalleh, S.R.; (2008). Electrocatalytic oxidation of methanol on carbon paste electrode modified by nickel ions dispersed into poly (1, 5-diaminonaphthalene) film. Electrochim. Acta, 53: 2402–2407.

Mojovic, Z.; Mentus, S.; Krstic, I.; (2007). Thin layer of Ni-modified 13X zeolite on glassy carbon support as an electrode material in aqueous solutions. Russ. J. Phys. Chem. A, 81: 1452–1457.

Azizi, S.N.; Ghasemi, S.; Chiani, E.; (2013). Nickel/mesoporous silica (SBA-15) modified electrode: An effective porous material for electrooxidation of methanol. Electrochim. Acta,88: 463–469.

Laviron, E.; (1979). General expression of the linear potential sweep voltammogram in the case of diffusionless electrochemical systems. J. Electroanal. Chem., 101: 19–28.

Luo, H.; Shi, Z.; Li, N.; Gu, Z.; Zhuang, Q.; (2001). Investigation of the electrochemical and electrocatalytic behavior of single-wall carbon nanotube film on a glassy carbon electrode. Anal. Chem., 73: 915–920.

Zheng, L.; Zhang, J.-Q.; Song, J.-F.; (2009). Ni (II)–quercetin complex modified multiwall carbon nanotube ionic liquid paste electrode and its electrocatalytic activity toward the oxidation of glucose. Electrochim. Acta, 54: 4559–4565.

Bard, A.J.; Faulkner, L.R.; (1980). Electrochemical methods: fundamentals and applications. John Wiley & Sons, New York.

Taraszewska, J.; Rosłonek, G.; (1994). Electrocatalytic oxidation of methanol on a glassy carbon electrode modified by nickel hydroxide formed by ex situ chemical precipitation. J.Electroanal. Chem., 364: 209–213.

Koper, M.; Hachkar, M.; Beden, B.; (1996). Investigation of the oscillatory electro-oxidation of formaldehyde on Pt and Rh electrodes by cyclic voltammetry, impedance spectroscopy and the electrochemical quartz crystal microbalance. J. Chem. Soc. Faraday Trans., 92: 3975–3982.

Zhao, C.; Li, M.; Jiao, K.; (2006). Determination of formaldehyde by staircase voltammetry based on its electrocatalytic oxidation at a nickel electrode. J. Anal. Chem., 61: 1204–1208.

Allen, J.B.; Larry, R.F.; (2001). Electrochemical methods: fundamentals and applications. John Wiley & Sons, New York.

Greef, R.; Peat, R.; Peter, L.; Pletcher, D.; Robinson, J.; (1985). Instrumental Methods in Electrochemistry. Chichester, England: Ellis Horwood Ltd.

AUTHOR (S) BIOSKETCHES

Mostafa Rahimnejad, Ph.D., Assistant Professor, Biofuel & Renewable Energy Research Center, Faculty of Chemical Engineering, Babol University of Technology, Babol, Iran.P.O.Box: 47148-71167, *E-mail: rahimnejad@nit.ac.ir*

Seyed Karim Hassaninejad-Darzi, Ph.D., Assistant Professor, Research Laboratory of Analytical & Organic Chemistry, Department of Chemistry, Faculty of Science, Babol University of Technology, Babol, Iran